

Synthesis and Characterization of Poly (3,5-Dimethylphenylacrylate) in Toluene at 40°C by Two-Angle Light-Scattering and Differential Pressure Viscometry

Nasrollah Hamidi

Department of Biological and Physical Sciences
South Carolina State University
Orangeburg, SC 29115
United States of America

Abstract

3,5-dimethylphenyl acrylate (35DMPA) was synthesized and chartered by GC-MS, NMR and density measurements. Poly(3,5-dimethylphenyl acrylate) (35PDMPA) was synthesized by radical polymerization of 35DMPA, fractionated to eleven samples of narrow molecular mass and chartered by NMR, and onlinetwo-angle (7° and 90°) light-scattering, and viscometry measurements with a size exclusion chromatographer. To characterize each sample, various volumes (15 μL to 150 μL with an interval of 20 μL) of dilute solutions (1-2 g/L) were injected to the SEC by autosampler from a 200 μL loop. The values of dn/dc , M_w , M_n , M_z , I , intrinsic viscosity, hydrodynamic radius, gyration radius, Kuhn-Mark-Houwink-Sakurada α and K-M-H-S K_α of each trail was estimated by Omniseq 4.2 program. Graphs of the above characteristic parameters of each trial against the amount of polymer injected showed that these values are slightly depending on the volume of polymer solution injected. The dimensions of 35PDMPA chains are scaled to their molar masses $R_h = 0.01289M_w^{0.5547}$. Double logarithmic relation of averages of M_w and $[\eta]$ shows the slope $\alpha = 0.650$, and intercept $K_\alpha = 0.0129$. The value of $\sigma = 2.47$ to 3.15 obtained from intercepts of Stockmayer-Fixman plot. It has been related to the chemical structure of the 35PDMPA and shear rate of viscosity detector

Introduction

The combined on-line measurement of intrinsic viscosity and two-angle (7° and 90°) light scattering (LS) with a gel permeation chromatography yields some of the most useful information to investigate the characteristics of polymer molecules in solution. Reproducibility of the measurements of a two-angle LS and its fundamental theory was presented by Terano and Mays.¹ The advantage of the method is clear since a single measurement yields much useful information about shape and form of macromolecules. Among them are: weight-average molecular weight (M_w), number-average molecular weight (M_n), z-average molecular weight (M_z), p-average molecular weight (M_p), polydispersity index $I = M_w/M_n$, intrinsic viscosity $[\eta]$, radius of gyration (R_g), hydrodynamics radius (R_h), Kuhn-Mark-Houwink-Sakurada (K-M-H-S) α , K-M-H-S K_α , and dn/dc .

Intrinsic viscosity is known to be a measure of overall static properties such as dimensions of a macromolecule. The intrinsic viscosity, by the means of statistical mechanics such as two parameters theories known as Stockmayer-Fixman method²⁻³ has been related to static dimensions of macromolecules. Traditionally, the intrinsic viscosity measured with a capillary viscometer. In this work the intrinsic viscosity of samples were estimated by a Viscotek four capillary, differential Wheatstone bridge viscometer at 40°C.

Estimation of the molar mass of a polymer is of considerable importance as the chain length can be a controlling factor in determining solubility, elasticity, fiber forming capacity, tear strength, and impact strength in many polymers.⁴ Absolute methods are classified by the type of average they yield such as colligative techniques; for example, membrane osmometry measures number average (M_n), light scattering yields weight average (M_w), and ultracentrifuge determines z-average molar mass (M_z).⁵ The absolute methods require extrapolation to infinite dilution for rigorous fulfillment of the requirements of theory.^{5,6} Relative methods such as size exclusion chromatography (SEC), viscosity, and vapor pressure osmometry require calibration with the samples of known molar masses. In this work a combination of two-angle light scattering⁷ with SEC used to estimate M_n , M_w , and M_z . The influence of side chain groups on the physical properties of polyethylene chains is well documented⁸. In the case of polyacrylates interests have focused on the changes induced by altering the length of alkyl ester group⁹ or identity of the ester linkage such as phenyl with alkyl substituent in various positions¹⁰.

One way to evaluate and analyze the properties of such polymers is to correlate the dependence of their equilibrium configuration to their structure. Among the methods of evaluating configurational properties are the application of two parameters theories such as K-M-H-Sand Stockmayer-Fixman relationship to viscosity and molar weight data to calculate conformational properties such as Flory's characteristic ratio (C_∞)¹¹ and or application of the wormlike model based on Yamakawa-Fujii theory¹² and its simplified form by Bohdaneky¹³.

The equilibrium properties of 35PDMPA were not published. Therefore this work presents experimental findings pertaining to the dilute solution properties of 35PDMPA polymer using on-line two-angle light-scattering to determine M_w and a differential pressure viscometer to evaluate intrinsic viscosity. The intrinsic viscosity in conjunction with the molecular mass data of 35PDMPA solutions are evaluated simultaneously and the data are treated according to the theories of intrinsic viscosity of random flexible polymers.

2. Experimental

2.1. Materials

3,5-dimethylphenol (35DMP) was purchased from Sigma-Aldrich; acryloyl chloride, hexanes, triethylamine, tetrahydrofuran (THF) were purchased from Fisher Scientific. Other solvents and reagents were purchased from the above mentioned companies. They were used without further treatments except toluene that was distilled before use.

2.2. 3,5-dimethylphenylacrylate

3,5-dimethylphenylacrylate (35DMPA) was synthesized by the reaction of acryloyl chloride and corresponding phenol in the presence of triethylamine and hexanes at low temperature in an ice-water bath. The solvent was extracted from filtrate by reduced pressure evaporator. The mixture of phenol and phenylacrylate were purified by fractional distillation under reduced pressure and three times re-distillations in the presence of hydroquinone (to stop heat induced radical polymerization). The 35DMPA was characterized by mass spectroscopy (GC-MS), IR and NMR.

2.3. Poly(3,5-dimethyl phenyl acrylate) Synthesis and Fractionation

35DMPA (15g) was polymerized in bulk with radical initiator 2,2'-azobisisobutyronitrile (~ 0.02% of monomer) under nitrogen flow for 2 hrs at 60° C. The obtained polymer was dissolved in dichloromethane, re-precipitated in hexanes three times, dried under vacuum (~5 torr) at 298 K for a week. A successive precipitational fractionation was carried out on the crude polymer by using dilute toluene solution of 35PDMPA (~2%) and hexanes as precipitants. Eleven fractions were obtained. Each sample was characterized by H-NMR and ¹³C-NMR in CDCl₃ and online measurements

2.4. Measurements

The solutions were prepared gravimetrically by measuring mass of solvent and solute using a Mettler-Toledo XS205 DoulRange analytical balance with an uncertainty of 0.01 mg. Redistilled toluene was used as mobile phase with rate of 0.50 mLmin⁻¹.

2.4.1. The Triple Detector Array (TDA)

The dilute solution viscosities were measured by Viscotek (Houston, TX) GPC-MAX 303 using various volume of the solution of a given sample of 35PDMPA in toluene. The injected volumes were from 15 to 150 μL with an interval of 10-20 μL (15, 25, 35, 75, 95, 110, 130, 150) μL.

TDA consists of a 18 microliters cell with a laser light at 760 nm, two-light scattering detectors, one at right angle and the other at low angle (~7°), a refractive index deflection type detector with reference cell volume 12 microliters and light emitting diode (LED) at 660 nm wavelength, and a four capillary, differential Wheatstone bridge configuration viscometer with bridge volume about 72 microliters. At a flow rate 3.0 mL/min THF, the shear rate = 3000 sec⁻¹. The SEC was equipped with two Viscogel-I series mixed bed columns, I-MBLMW-3078 for low molar mass polymer and I-MBHMW-3078 for resolution of higher molar mass polymers. All detectors are housed in a thermostat oven.

2.4.2. GPC Autosampler

The Viscotek GPC autosampler uses a fixed 200 μL volume sample loop with variable injection volume syringe.

It was programmed for two washafter each injection, and purging RI and DP cells five min before each injection. The standard 2 mL clear glass, screw cap vials were filled with the sample then located in the corresponding vial rack number. Both detector and autosampler controlled by a Dell PC running Omniseq 4.2 software

2.4.3. Densitymeter.

The densities of 35DMPA were measured by a DMA-5000 Anton Parr (Graz) density meter which was calibrated with air and triple distilled water prior to measurement at 20.00 °C. The DMA 5000 density-meter determines the density based on measuring the period of oscillation of a vibrating U-shaped hollow tube that is filled with the sample¹⁴. The measurements were run in the slow equilibrium mode (about 5 min equilibration) to ensure the highest possible quality of data. The accuracy of the data was estimated from the average deviation between the data sets. Evaporation was prevented by capping the ends of the U-tube. Also, frequently, the tube was checked for formation of small bubbles which lead to an increasing error on the measured data. For pure water the inaccuracies of the density measurements estimated not exceeding 0.000005 gcm⁻³ and for organic liquids 0.000010 gcm⁻³ at 20.00 °C.

Results and Discussion

3.1. 35DMPA Characterizations

GC-MS. Fig 1 shows the mass fragmentation of 35DMPA obtained from a Perkin-Elmer GC-MS. The mother ion showed at M/z =176 corresponding to 35DMPA, M/z = 122 corresponding to phenol itself, and the base ion at M/z = 55 corresponding to [C₃H₃O]⁺ as expected

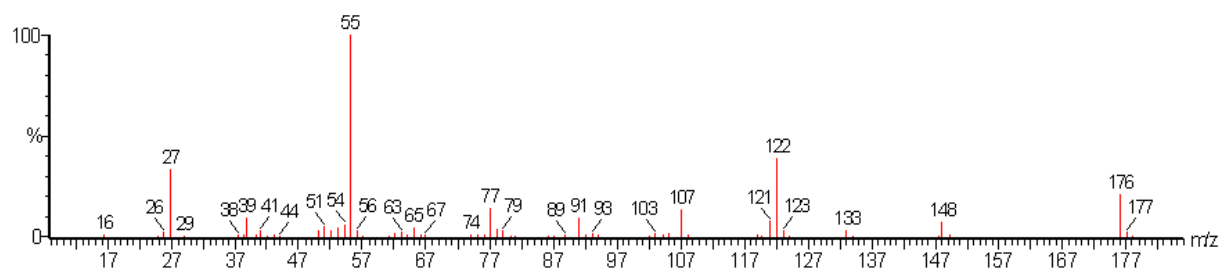


Fig 1. Mass spectrometry of 35DMPA.

¹H-NMR. The ¹H-NMR of 35DMPA taken by a 400 MHz Spectrophotometer at room temperature. The resonance of 35DMPA in unit of δ ppm are: 6.73 s (2 Ar-H), 6.54 s (1 Ar-H), 6.53-6.60 two doublet, (1 H-C=C-H₂) 6.34-6.24 four singlet (1H-C=C-H₂), 5.97-5.91 two doublet of doublet (1H-C=C-H₂), 2.30 s (6HAr-CH₃).

¹³C-NMR. The ¹³C-NMR of the 35DMPA in CDCl₃ (chloroform signal 77.51, 77.19, 76.87 ppm and TMS at zero ppm) shows the ester carbonyl carbon, the vinyl carbons resonance at 165.15, 155.99 and 150.43 ppm and the aromatic carbons resonance at 139.31, 132.57, 127.69, 121.96, 119.07, 113.16 ppm. The methyl carbons attached to aromatic ring resonance at 21.21 and 21.15 ppm.

Density. Figure 2 shows the variation of density of the 35DMPA by temperature from 4° C to 50°C. The best line fitted to the data by least square is $\rho = -.000856(t^\circ) + 1.044217$ mL/g. The calculated density for 35DMPA by group contribution based on van Krevelen and Hoftyzer at 25°C is 1.060 g/mL which is near to experimental value of 1.023 g/mL.

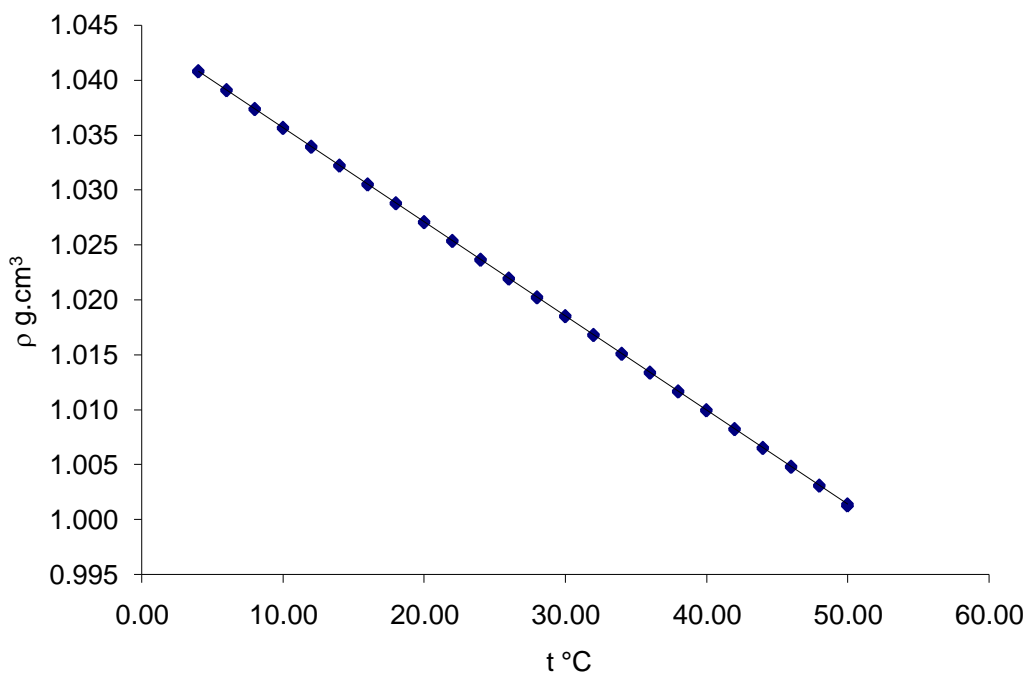


Fig 2. Variation of density of 35DMP with temperature from 4 °C to 50 °C

3.2. 35PDMPA Characterization

¹H-NMR. Figure 3a shows 400 Mz¹H-NMR of the 35PDMPA sample F9 in CDCl₃ chloroform ($\delta = 7.286$ ppm). The signals at $\delta = 6.8$ ppm and $\delta = 6.7$ ppm are assigned to para and ortho-protons in the phenyl side chain with relative abundance 1:2 –H as expected. The multiplet from $2.0 < \delta < 2.2$ belong to the m-methyl hydrogen on the benzene ring side chain. The broad signal centered at $\delta = 2.5$ ppm belong to methyne backbone and the other broad signal at $\delta = 3.0$ ppm belongs to methylene backbone with the relative area 2:1 as expected. Only one of the samples showed a broad signal between 1.78 and 1.4 ppm centered at $\delta = 1.6$ that belongs to moisture which may exist as impurity in CDCl₃; this was confirmed by deuterium exchange experiment. The resonance centered at $\delta = 1.6$ shows in Fig 3a. It was disappeared by D₂O exchange as shows Fig 3b.

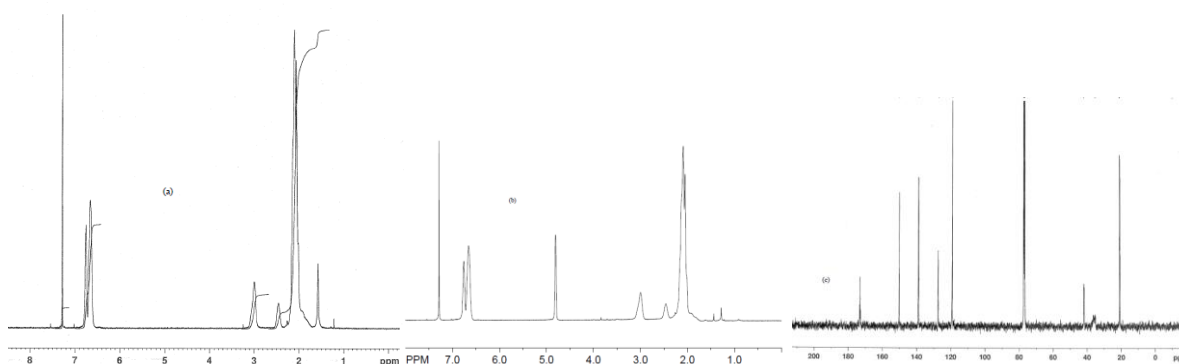


Fig 3.(a) 400 Mz¹H-NMR of the 35PDMPA in chloroform (b) D-exchange of the same and (c) ¹³C-NMR of the 35PDMPA ind-chloroform.

¹³C-NMR. Fig 3c shows a ¹³C-NMR of 35PDMPA in CDCl₃ (chloroform $\delta = 76.71-77.34$ ppm). The ester carbonyl carbon resonances at 173.23 ppm and the aromatic carbon attached to the oxygen atom gave signal at 150.36 ppm. The aromatic carbon atoms to which methyl groups are attached gave resonance signals at 139.08 and 139.16 ppm. The other aromatic carbons gave signals at 119.25, 119.17 and 127.50 ppm. The backbone methylene carbons give signals at 41.90 and methyne give a multiple centered at 34.0-37.6 ppm respectively. The resonances at 20.94 and 20.89 ppm are attributed to the methyl carbons attached to the aromatic nucleus

4. On-Line Characterizations

4.1. Standard Polystyrene in Toluene at 40°C.

Fig 4a shows variation of RI responses versus amount of polystyrene (PS) sample in toluene at 40°C. From the graph the values of dn/dc of PS in toluene at 40°C was determined to be 0.10855; which is within expected value.

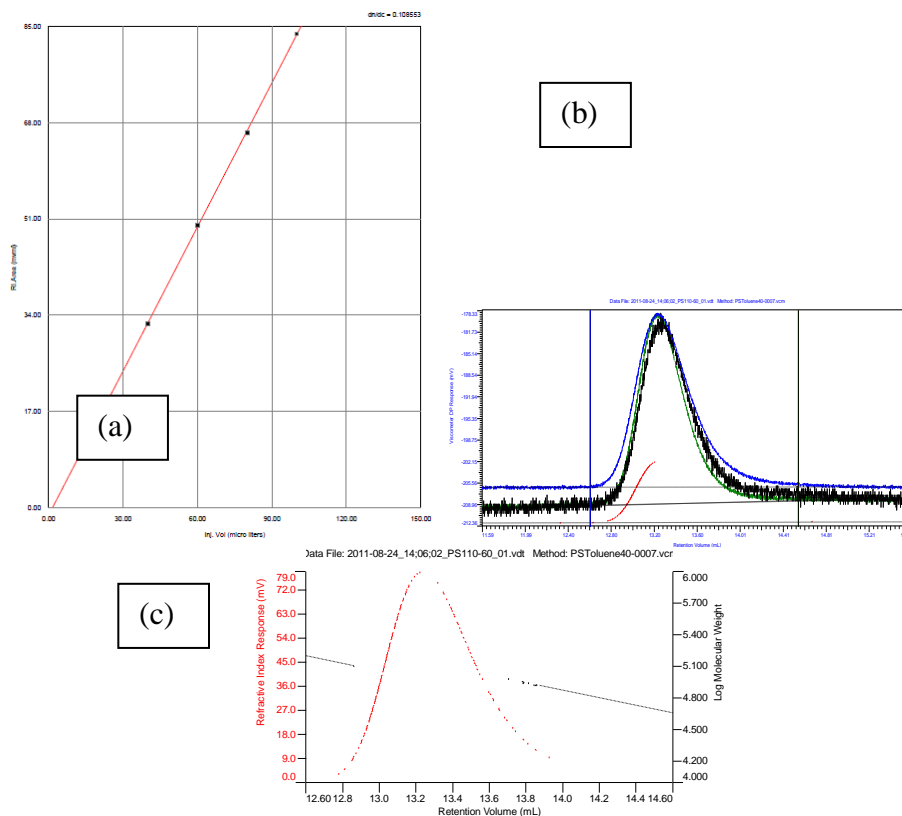


Fig 4(a) Variation of RI responses versus amount of PS sample in toluene at 40°C (b) Chromatograms of polystyrene standard samples after normalization: $M_{w,ls} = 110,000$, $M_w/M_n = 1.06$. From top to bottom (blue) differential pressure viscometer, (green) right angle light scattering, (black) low angle light scattering, (red) refractive index. (c) Refractive index versus retention time and LogMw of standard polystyrene sample versus retention time.

Fig 4b shows the four chromatograms of polystyrene standard samples $M_{w,ls} = 110,000$ with $M_w/M_n = 1.06$ each coming from a given detector, from top to bottom: DP, RALS, LALS, and RI detectors after normalization. The molecular parameters obtained from the chromatograms agreed well with the accepted values.

Fig 4C contains two graphs one showing the refractive index versus retention time and the other shows variation of LogMw of standard polystyrene sample versus retention time. The almost flat line of molecular mass by retention time indicates the sample is monodisperse polymer as was expected.

4.2. On-Line Solution Properties of 35PDMPA in toluene at 40°C

4.2.1. Refractive Index Increment.

The accuracy of molecular weight determination by light scattering is highly dependent on refractive index increment (dn/dc), an optical property of the polymer solution. Refractive index increment is the rate of change of refractive index versus the concentration of the solution at a given temperature and a given wavelength of the light which varies from solvent to solvent. Typically high refractive index increment values indicate better optical property resulting in good light scattering detector signal/noise and more accurate data calculation. Accurate dn/dc values can be obtained by plotting the refractive index of the polymer solution versus varying solution concentration as indicated in figures below. Fig. 5 shows the areas under the refractive index signal versus concentration including the best fitted line to the experimental data.

The dn/dc obtained from Fig 5 for each sample of 35PDMPA are near to each other. The last plot of Fig 5 shows a graph of variation of dn/dc versus M_w ; a straight line with a very small slope and the intercept near to mathematical average of the dn/dc values fitted well by least-square method into experimental data.

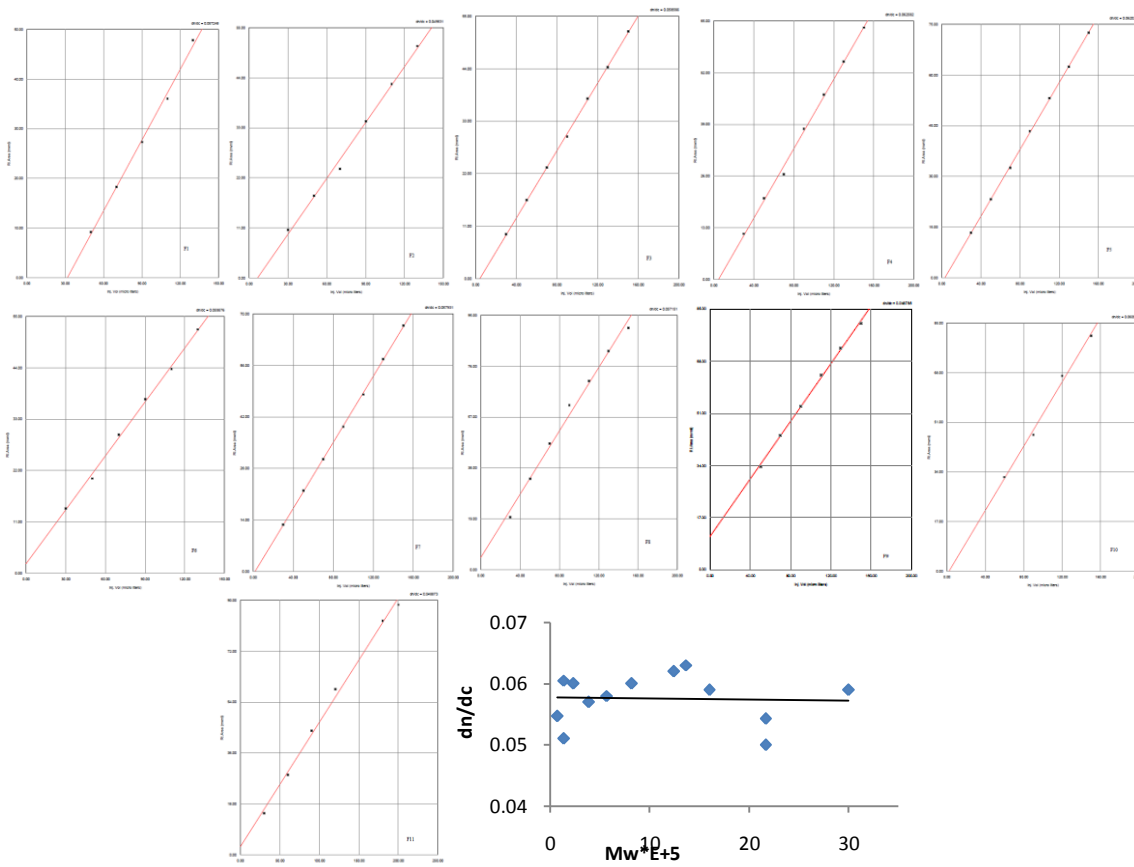


Fig 5. Estimation of refractive index increment (dn/dc) by plotting the variation of refractive index responses versus concentration of samples of 35PDMPA in toluene at 313.15 K. The last graph shows dn/dc of each sample as a function of M_w .

Fig 5 shows there is no dependence of refractive index increment by molecular weight of 35PDMPA in toluene at 40°C. Therefore, it will be appropriated to take an average value of dn/dc to evaluate M_w of the 35PDMPA and toluene system.

4.2.2. Chromatograms of 35PDMPA in Toluene.

The molar mass of the polymer samples were estimated by on-line two-angle light scattering using the chromatograms data with the average value of $dn/dc = 0.0576$ for all samples in the Omnisec program. Fig 6 shows a sample of chromatogram for each fraction of polymer registered data from four detectors: DP, RALS, LALS, and RI. All are clean of sparks and symmetric as was expected.

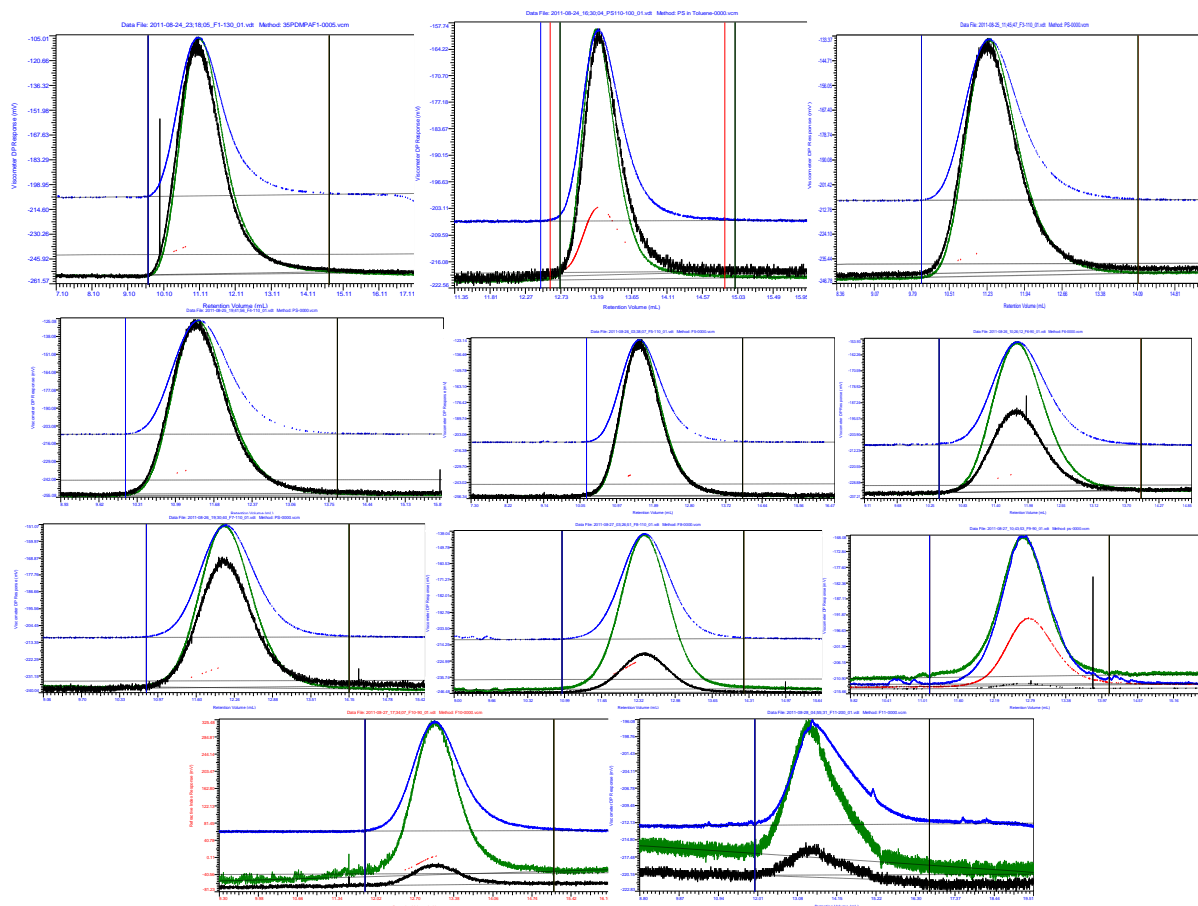


Figure 6. DP, RALS, LALS, and RI chromatograms of samples of 35PDMPA in toluene at 40°C

4.2.3. Molecular weight distribution of 35PDMPA in Toluene.

Fig 7 contains 11 diagrams belonging to eleven samples of 35PDMPA; each having two graphs, one refractive index responses versus retention time and the other is $\log M_w$ of sample versus retention time. All samples show a uniform distribution of molar mass except the two samples coming from the ends of fractionation procedure. These two samples showed a different molar mass distribution. The sample F1 has more of higher end M_w polymer as one would expect of a head fraction of precipitation fractionation method and sample F11 possess more of lower molar mass polymer as anticipated. Other samples have a uniform distribution of the molar mass as one assumes.

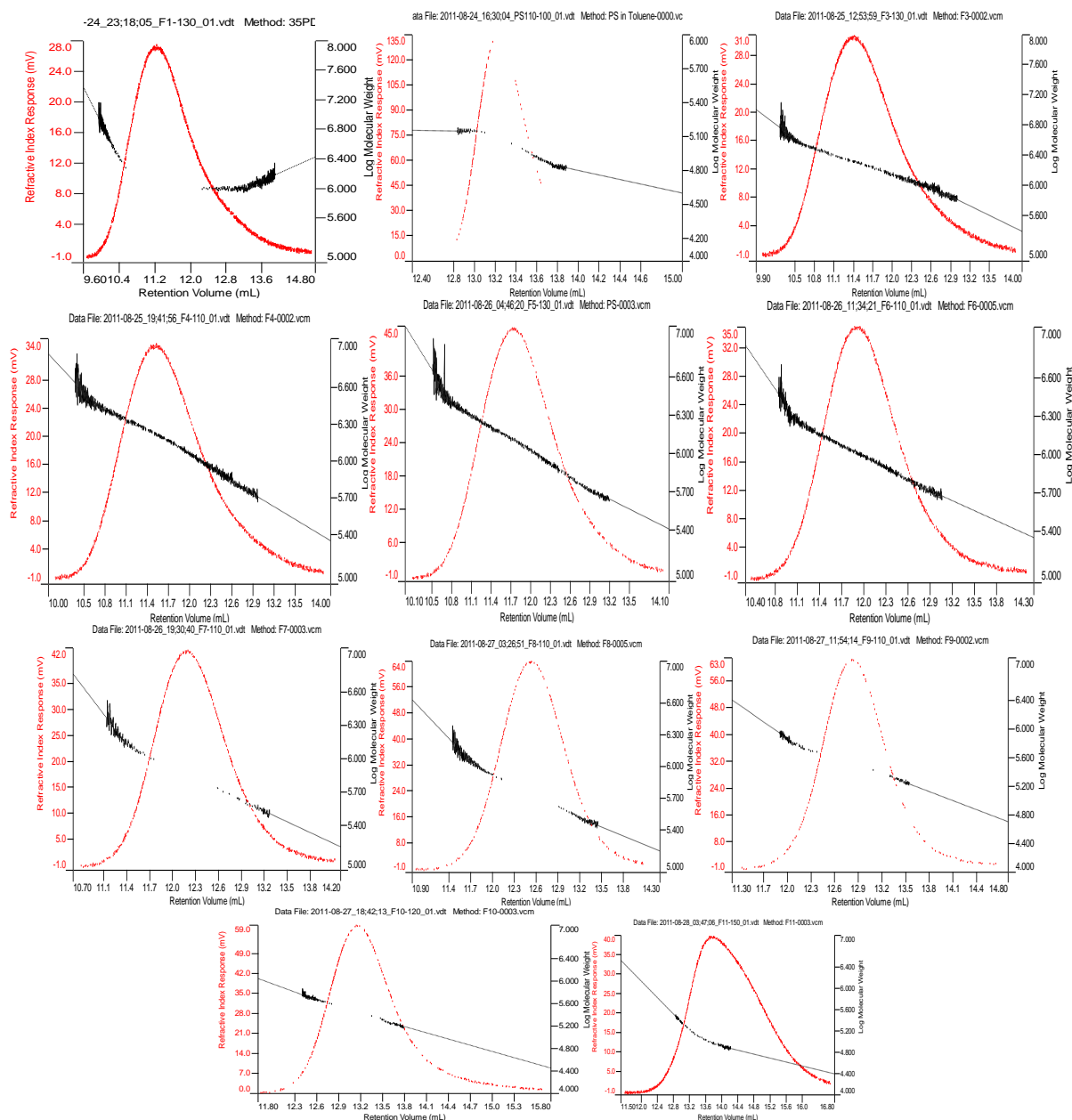


Figure 7. Refractive index versus retention time and molar mass of 35PDMPA versus retention time.

4.2.4. Molecular Weight and concentration of 35PDMPA

Table 1 contains the characteristic parameters of eleven samples of 35PDMPA in toluene at 40°C. The reported molar mass on the Table 1 for each sample is the average of five to eight trials. Fig 8a shows the Mw of each trial versus the amount of polymer content of each sample. There is an evidence of concentration dependence of molar mass which is not within expectation. Since the expectation is that the two-angle light scattering gives absolute molar mass.

Table 1. Molecular parameters of 35PDMPA in toluene at 40°C

Sample	F1	F2	F3	F4	F5	F6	F7	F8	F9	F10	F11
Peak (mL)	11.16	11.21	11.35	11.45	11.68	11.90	12.21	12.55	12.80	13.17	13.81
MnMDa	3.04	1.64	1.61	1.39	1.11	0.872	0.631	0.444	0.299	0.157	0.053
Mw MDa	3.65	2.10	2.10	1.74	1.38	1.02	0.732	0.512	0.348	0.198	0.098
MzMDa	4.34	2.47	2.48	2.06	1.62	1.16	0.840	0.582	0.405	0.237	0.168
MpMDa	4.22	2.37	2.39	1.97	1.46	1.07	0.740	0.504	0.347	0.206	0.094
Mw / Mn	1.20	1.28	1.30	1.26	1.24	1.17	1.16	1.15	1.17	1.27	1.97
IV (dL/g)	2.28	1.44	1.64	1.46	1.32	1.11	0.90	0.70	0.53	0.35	0.21
Rh (nm)	49.7	35.6	37.2	33.7	30.1	25.8	21.5	17.6	14.1	10.1	6.5
Rg (nm)	67.7	54.8	46.9	41.8	35.0	30.0	25.0				
M-H a	0.719	0.569	0.673	0.602	0.839	0.706	0.728	0.760	0.697	0.776	0.586
K*E-3	0.04	0.37	0.09	0.26	0.01	0.06	0.05	0.03	0.07	0.03	0.256

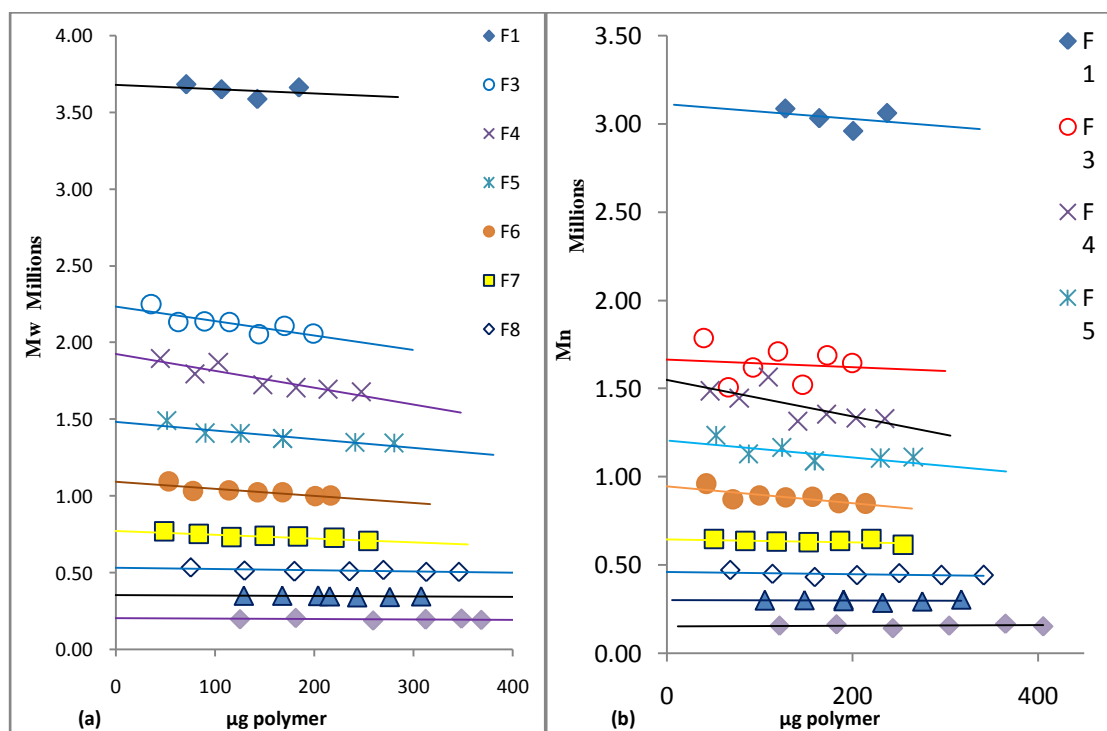


Fig 8. (a) Variation of Mw by the amount of sample (concentration x volume injected) of polymer by light scattering measurements. (b) Variation of Mn by the amount of polymer determined Omnisecc program calculations

Also, the Mn was calculated by the Omnisecc program using the RI data at each chromatogram. Fig 8b shows the concentration dependence for Mn as estimated by Omnisecc program. At lower volume of sample injected the polymer molecules behave like to be at a lower concentration, therefore the polymer expands more, thus a higher volume and molar mass of the polymer is detected.

4.2.5. Hydrodynamic and Gyration Radius of 35PDMPA

The Omnisecc 4.2 program also estimates the value of radius of gyration (R_g) of a sample. Fig 9a shows the variations of R_g of the samples of 35PDMPA in toluene at 40°C versus the amounts of polymer. As individual graphs show there is a dependence of radius of gyration versus the amount of the polymer sample. However, this dependence is not uniform as was the case of Mw, Mn and intrinsic viscosities.

The concentration of sample has not been changed; the injection volume has been increased, therefore the amount of sample reaches to detectors increases. This could be interpreted as increasing the concentration of polymer in the sample; it understandable that at lower concentrations the effects of excluded volume will be higher and hence a higher R_g may be observed.

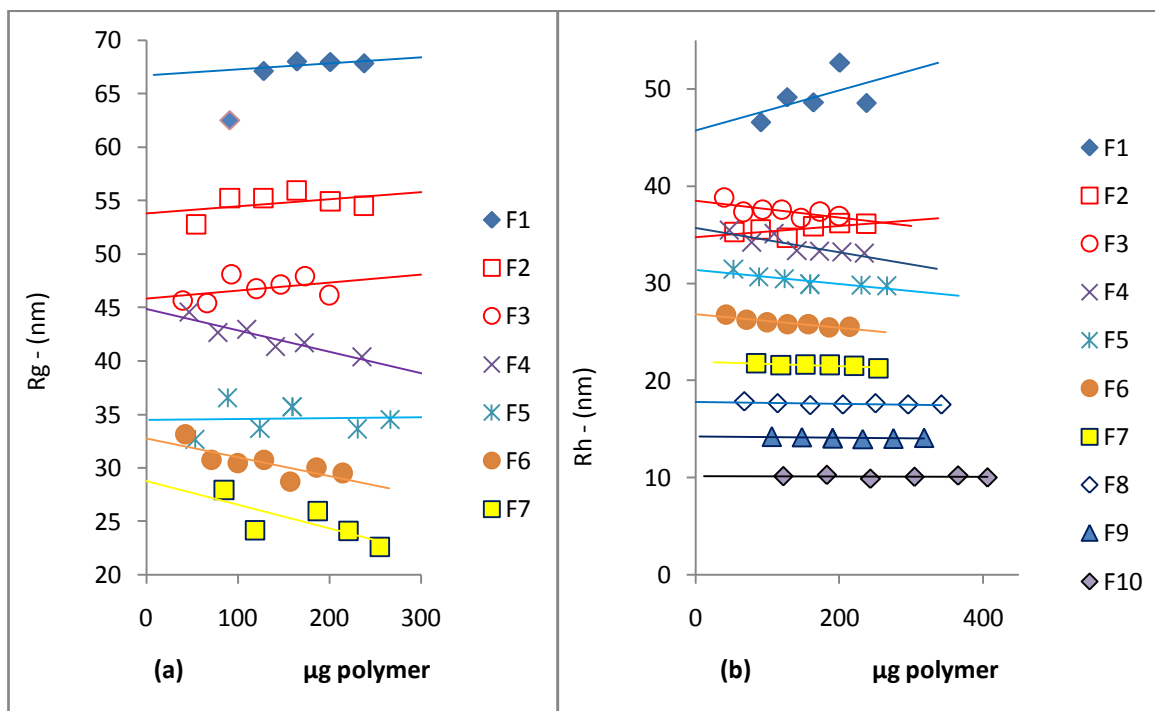


Fig 9.(a) Variation of R_g by amount of polymer and (b) Variation of R_h by concentration of polymer.

Also, the Omnisec4.2 estimates the hydrodynamic radius (R_h) of the polymer sample. Fig 9b shows the hydrodynamic radius of the polymer sample versus the amount of polymer sample injected into the GPC system. As the Fig 9b indicates the hydrodynamic radius depends on amounts of the sample. For all samples the R_h increases with decreasing the amount of the polymer except for samples F1 and F2 that the R_h decreases with decreasing the amount of polymer. Therefore the effects of excluded volume in the very high molar mass were not as strong as in lower molar mass polymers.

4.2.6. α and K_α of 35PDMPA

The Omnisec 4.2 program estimate values of slope and intercept of K-M-H-S for each sample. Fig 10a shows the variation of α , the K-M-H-S exponent estimated for individual samples versus the amounts of the polymer. The value of α also depends on the sample and the amounts of polymer; this is not within anticipation. The values falls between 0.52 to 0.85; this is expected values for random coil polymers. A dependence on K-M-H-S α and the amount of polymer sample was observed as Fig 10 shows. Five trials were measured for sample F1; three trials showed a value of α within expectation ($0.5 < \alpha < 0.8$); however two trials showed a value of $\alpha > 1$ (e.g. 3.4 and 4.3) which are not within anticipation. All samples showed dependence of α on the volume of polymer injected which is not within expectation.

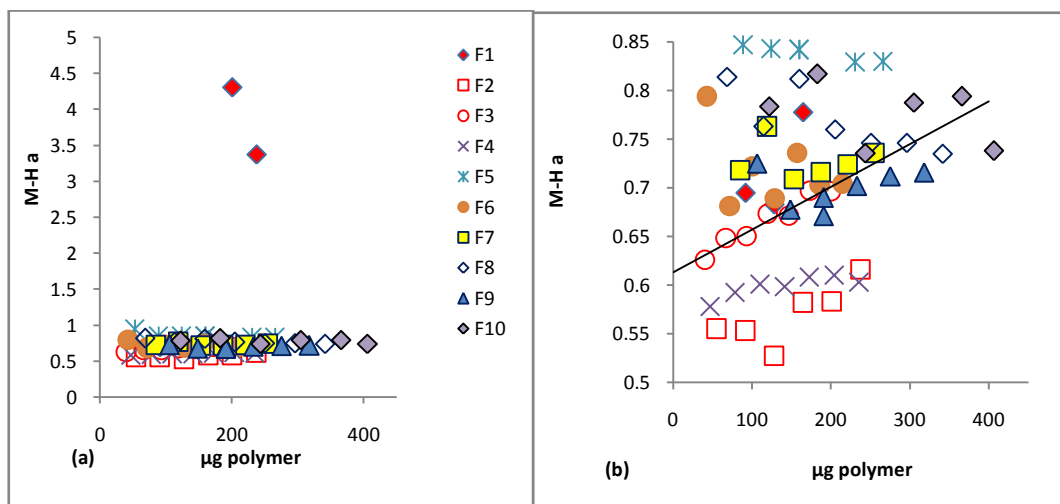


Fig 10.(a) Variation α of each sample by concentration of polymer. (b) Expansion of a section of Fig 10 (a)

Fig 11 shows the variation of K_a versus the amount of polymer showing K_a value of each trial of a sample. The value of K_a of all sample and all trials must be agreed within standard deviations, however, for most of samples as the amount of polymer injected decreases the value of K_a increases.

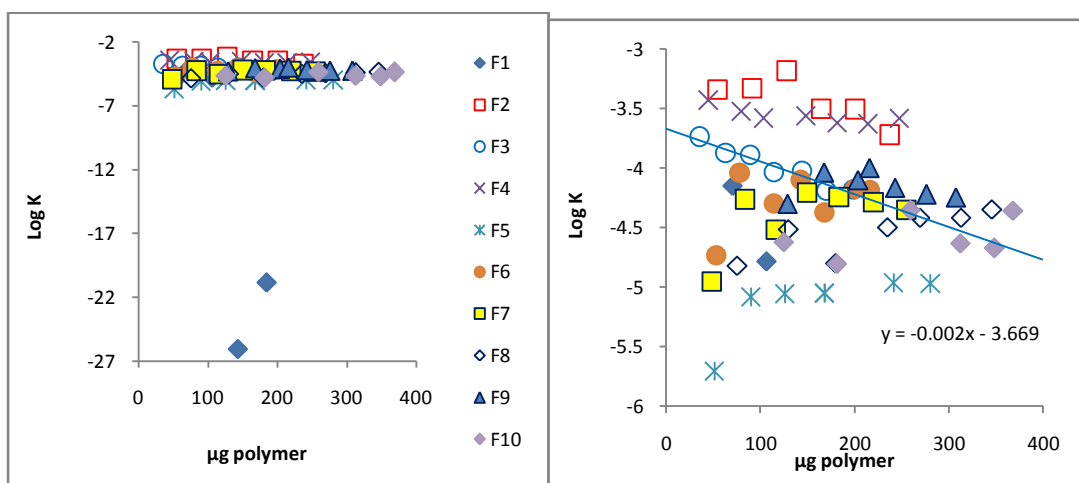


Fig 11. Variation of K-M-H-S K_a by the amounts of polymer

Over all every measured property was depending on the volume of the injected polymer. This is within expectation since the absolute methods require extrapolation to infinite dilution for rigorous fulfillment of the requirements of theory.

4.5. Characteristics Parameters as a Function of Molecular Weight

4.5.1. Dependence of R_g and R_h by molar mass of 35PDMPA

For flexible chain polymers, the radius of gyration $\langle R_g^2 \rangle^{1/2}$ is proportional to $M^{1/2}$ in the theta condition, but in good solvent the fog volume expands, so $\langle R_g^2 \rangle^{1/2} \sim \alpha M^{1/2}$ with α being the expansion factor. The expansion factor α is molecular weight dependent, so $\langle R_g^2 \rangle^{1/2} = k_v M^v$ in general. In a good solvent, both k_v and v are a function of the solvent quality and chain length. Fig 12 contains two graphs: (a) the double logarithmic variation of average of hydrodynamic radii values of each sample versus molar mass of the sample. The data well-described by the following power laws:

$$R_g = 0.00528 M_w^{0.6248} \quad (1)$$

$$R_h = 0.01289 M_w^{0.5547} \quad (2)$$

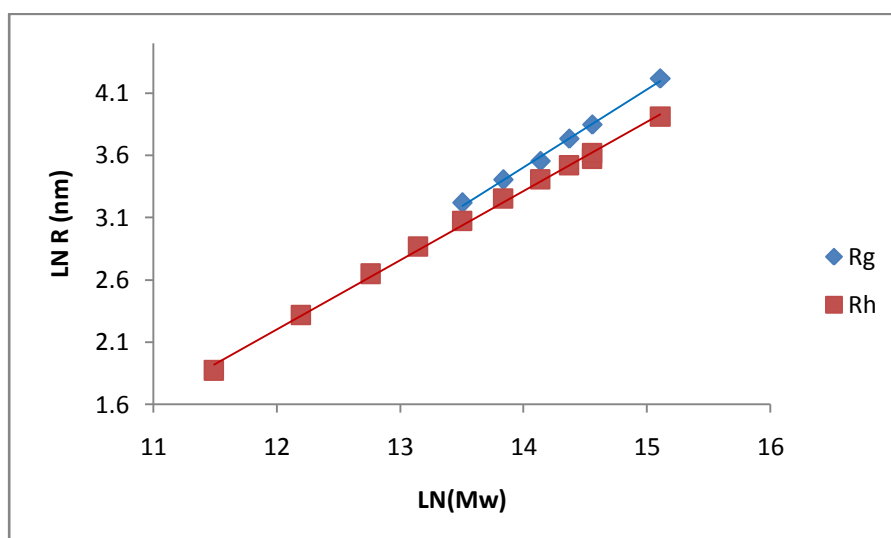


Fig 12. Radius of gyration and hydrodynamic radius as a function of molecular weight for 35PDMPA in toluene at 40 C

For monodisperse spheres viscometric, thermodynamic, and R_h radii are identical and larger than the R_g by a factor of $(5/3)^{1/2}$. For sufficiently long flexible chains in good solvents these radii are expected to differ from one another but to vary with molecular weight in the same way. According to Le Guillou and Zinn-Justin¹⁶ the $R_g \sim M^{0.588}$ in the asymptotic range of strong excluded volume effects, a predication that describes the neutron and light scattering data on polystyrene very well.¹⁷ For 35PDMPA the R_g exponent of Mw, 0.625 is higher than predicted by theory and the R_h exponent, 0.554₇ is lower than predicted value. These results are similar to observation of polystyrene in benzene in the sense that R_g exponent is higher than R_h exponent.¹⁸

The value of α in the K-M-H-S equation is equal to $(3\nu - 1)$.¹⁹ In a good solvent, the cloud swells because more solvent molecules are taken inside the cloud. Values of $\alpha = 3(.5547) - 1 = 0.664$ is near to 0.650, the exponent of KMHS equation.

4.5.2. Variation of K_α and α by molar mass of 35PDMPA

Fig 13 shows the variations of K_α and α of 35PDMPA versus Mw of the sample. The α and K_α are estimated by Omnisec program and were averaged for each sample. The least-square line that fits into plots of data has the slope of -0.0013 and intercept of $\alpha_0 = 0.713$. The variation of α by molar mass as shown in Fig 13 is not within expectation. Fig 13 also contains the variation of K_α versus Mw. The experimental data are scattered and the best least-square line fitted to the data has the slope of .0051 and intercept of 0.0466.

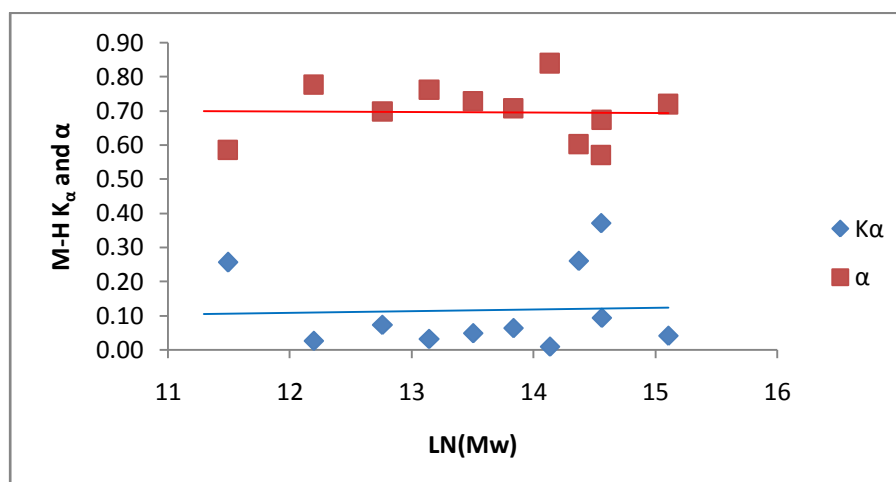


Fig 13. Variation α and K_α versus Mw of 35PDMPA in toluene at 40°C.

4.6. Intrinsic Viscosity of 35PDMPA

4.6.1 Intrinsic viscosity and concentration of 35PDMPA

The differential pressure viscometer in TAD is capable of measuring the absolute value of intrinsic viscosity. The Omniseq 4.2 program using the information of refractive index and concentration estimates the intrinsic viscosity of the polymer. Therefore the intrinsic viscosity obtained in this manner must not depend on the amount of polymer injected into SEC. However, as the graphs in Fig 14 shows there is a dependence of intrinsic viscosity with the amount of polymers. As the injected volume (concentration) of the polymer decreases a higher values of intrinsic viscosity observe. This means that the chain expands more in diluted solutions which is within expectation. The other factor that may affects the under estimation of intrinsic viscosity is the shear rate of the four capillary, differential Wheatstone bridge viscometer detector. The manufacturer estimates a shear rate of 3000 sec^{-1} when 3 mL/min THF passing through the system. The shear rate for 0.5 mL/min of toluene is much less than the indicated value, however, the existence of shear rate under estimates intrinsic viscosity up to several folds.²⁰

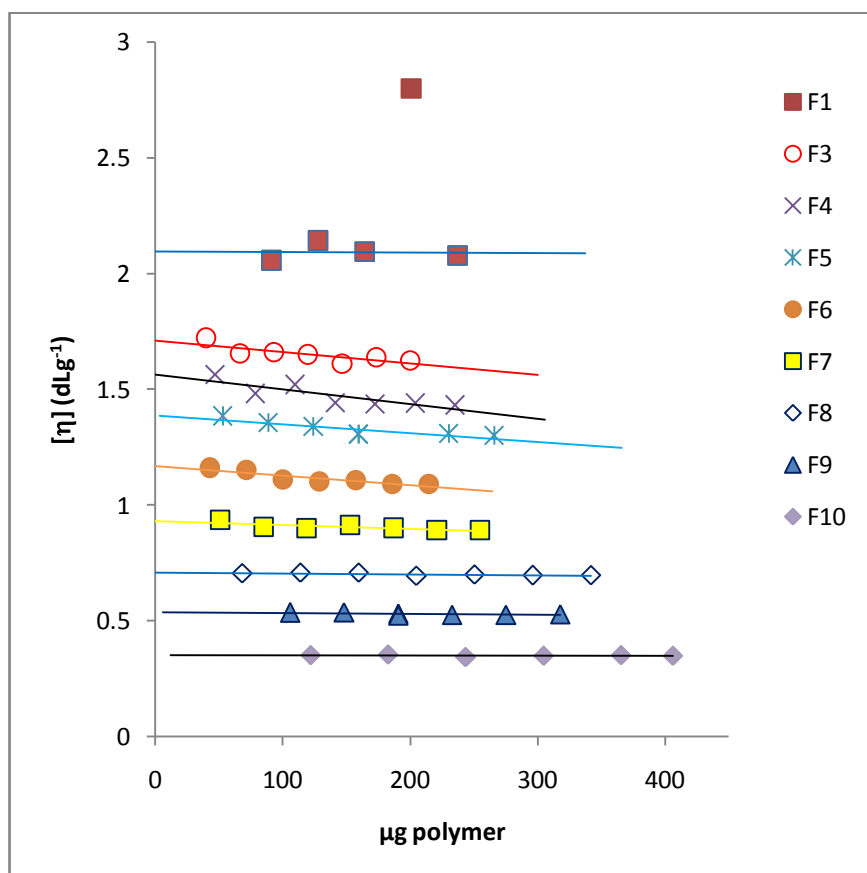


Fig 14. Variation of DP intrinsic viscosity by amounts of polymer.

4.6.2 The Intrinsic Viscosity and Molar Mass

The dimensions of a linear flexible polymer are obtained either by light scattering as one can see in Figure 12 or by dilute solution viscometry of macromolecules. The molecular weight dependence of $[\eta]$, are expressed in the values of K_α and α of K-M-H-S. Fig 15 shows the treatment of average intrinsic viscosity and Mw in the light of double logarithmic plot of K-M-H-S. The least-square line fits well into experimental data with exponent, $\alpha = 0.650$ and $K_\alpha = 0.0128_s$. Several factors contribute to enhance the exponent α .²¹ Among them are: (a) chain stiffness, (b) excluded volume, and (c) partial drainage. It is universally accepted that the value of α that corresponds to a nondraining coil unperturbed by the excluded volume effect is 0.5; this does not include the low-molecular mass region, and temperatures below theta condition where the values of α are found to be less than 0.5. Besides of the above mentioned parameters, the chain thickness is the only contributing factor that reduce the value of α ; in the limit of molecules having thickness equal to length (sphere), $\alpha = 0$.

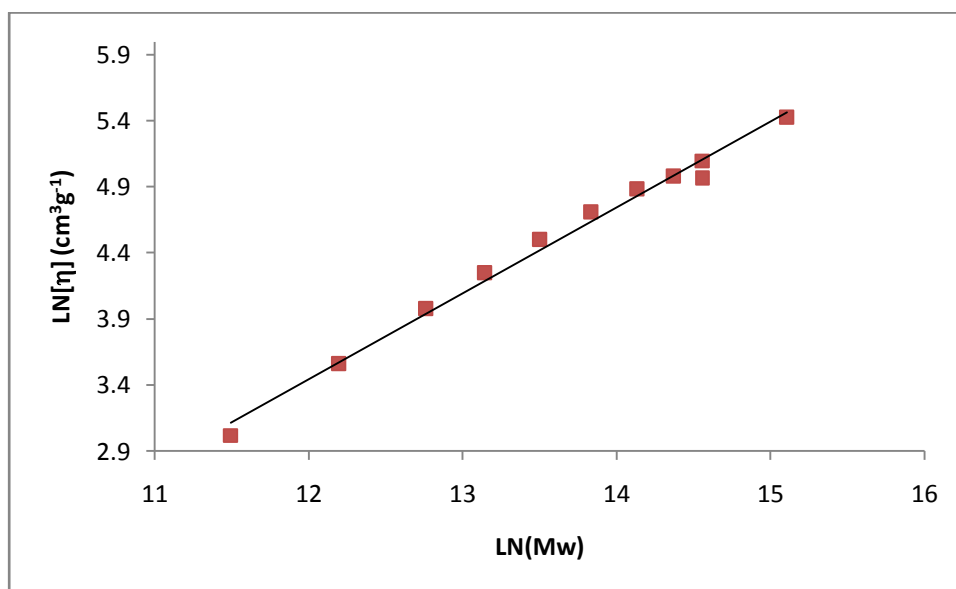


Fig 15. The double logarithmic plot of DP intrinsic viscosity and Mw of 35PDMPA.

4.6.3. Unperturbed Dimensions

The expansion of a covalently bonded polymer chain in solution is restricted by length of covalent bonds (l) and valence angles between each chained atoms (θ). In general the square of end-to-end dimensions $\langle R_{00}^2 \rangle$ independent of bond angle restriction expresses as nl^2 , which can be modified to allow for the short-range interactions produced by bond angle restrictions θ for a homoatomic C-C chain:⁴

$$\langle R_{0f}^2 \rangle = nl^2 \frac{(1 - \cos \theta)}{(1 + \cos \theta)} \quad (3)$$

For the simplest case of an all carbon backbone chain such as polyethylene, $\cos 109.5 \sim -1/3$ so that the Eq. (3) becomes:

$$\langle R_{0f}^2 \rangle = 2nl^2 \quad (4)$$

This indicates that the polyethylene chain is twice as extended as the freely jointed chain model when the short-range interactions are considered. In fact, in butane and carbon chains with more atoms, steric repulsions impose restrictions to bond rotations.²² This feature in equation (3) causes further modified:

$$\langle R_o^2 \rangle = nl^2 \frac{(1 - \cos \theta)(1 - \cos \langle \phi \rangle)}{(1 + \cos \theta)(1 + \cos \langle \phi \rangle)} \quad (5)$$

where $\langle \cos \phi \rangle$ is the average cosine of the angle of rotation of the bonds in the backbone chain. The parameter of $\langle R_o^2 \rangle$ is the average mean square of the unperturbed dimension, which is the main characteristic parameter of a polymeric chain.

For a 35PDMPA chain, the unperturbed dimension may be obtained directly from the intercept of the M-H-K-S plot, K_0 , in an ideal solution. In non-ideal solvents, such as case of 35PDMPA in toluene at 40°C, the unperturbed dimensions usually are estimated by extrapolation methods using a number of plots based on theoretical or semi-theoretical equations developed for this purpose, i.e., applications of the excluded volume equations between the molecular weight and intrinsic viscosities in good solvents. Stockmayer-Fixman⁹ proposed one such relationship for treating data covering the usual range of molecular weights encountered in experiments.

$$[\eta]M^{-\frac{1}{2}} = K_\theta + 0.346\Phi_0BM^{\frac{1}{2}} \quad 0 \leq \alpha^3 \leq 1.6 \quad (6A)$$

$$[\eta]M^{-1/2} = 1.05K_{\theta} + 0.287\Phi_0BM^{-1/2} \quad 0 \leq \alpha^3 \leq 2.5 \quad (6B)$$

Φ_0 is the Flory's universal viscosity constant, at infinite molar mass when $[\eta]$ expressed in mL/g, the theoretical value of $\Phi_{0,\infty}$ is $2.87 \times 10^{23} \text{ mol}^{-1}$.²³ Other values used for Φ_0 depending on molecular mass of the polymer and the kinds of polymer; with the best experimental value of 2.51×10^{23} to 2.87×10^{23} .²⁴

The constant K_{θ} of S-F is the intercept of the plot; it is equal to the MHKS' K_{α} at the theta conditions. . The K_{θ} is related to the unperturbed dimension of the polymer.⁴

$$K_{\theta} = \Phi_0 \left(\frac{\langle R_0^2 \rangle}{M} \right)^{3/2} \quad (7)$$

The expansion factor of 35PDMPA in toluene does not exceed 1.6 for the data; therefore equation (6A) is applicable in toluene. The plot of $[\eta]M^{-1/2}$ against $\langle M_w \rangle^{1/2}$ according to the Eq. (6A) for 35PDMPA in toluene is shown in Fig. 16.

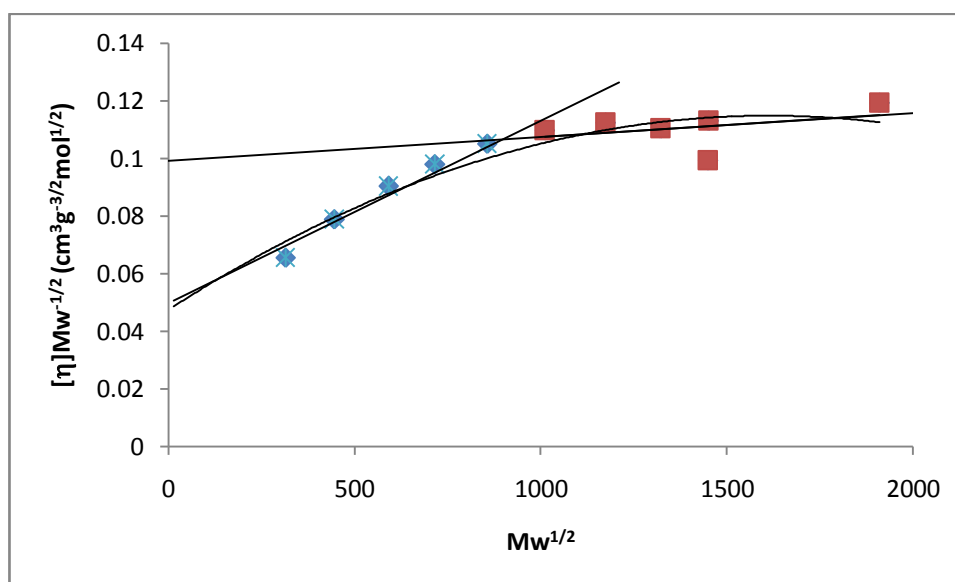


Fig 16. Stockmayer-Fixman plots for 35PDMPA fractions in toluene at 40°C.

The value of K_{θ} in toluene at 40°C is estimated by fitting a least-square straight line into data points. Table 2 shows the molecular parameters of 35PDMPA, poly(methyl acrylate) (PMA) at 40°C, and poly(3,5-dimethylphenyl methacrylate) (35PDMPMA) at 25°C. The least-square line fitted to all data gives $K_{\theta} = 0.0714$ which is lower than of PMA and 35PDMPMA. Moreover, as Fig 16 shows the data are not fitting well into a straight line, however, a second order polynomial curve fits well into data which produces a K_{θ} slightly smaller than previous one.

Also one may consider divide the graph into two sections: low and high molar mass regions. Comparisons 35DMPA's K_{θ} with 35PDMPMA and PMA indicate that the intrinsic viscosity has been underestimated at lower molar mass. The under estimation of intrinsic viscosity comes from the high shear rate of the four capillary, differential Wheatstone bridge viscometer detector. The existence of shear rate under estimates intrinsic viscosity by several folds. The highest under estimations of intrinsic viscosities happens at higher shear rate, i. e. lower molar mass region. This leads to smaller K_{θ} values and curvature of Stockmayer-Fixman plot.

Table 2. Values of K_0 , $(\langle R_0^2 \rangle / M)^{1/2} C_\infty$, slope of the line and B obtained from extrapolation of $[\eta]$ against $\langle M_w \rangle$ according to SF, along with $(\langle R_0^2 \rangle / M)_\infty^{1/2} C_\infty$, and σ .

Polymer	K_0	$(\langle R_0^2 \rangle / M)_\infty^{1/2}$	σ	C_∞	slopeE5	E.E23
35PDMPA All Data	0.0714	0.655	2.82	15.94	2.82	2.17
35PDMPA High Mw	0.0992	0.731	3.15	19.85	0.83	0.64
35PDMPA Low Mw	0.0497	0.581	2.50	12.53	6.34	4.89
35PDMPA 2 Order	0.0476	0.572	2.47	12.17		
PMA ¹	0.0951	0.721	2.17	9.43		
35PDMPMA ²⁵	0.1576	0.853	3.82	29.18		

The σ known also as the steric parameter for a complex chain, such as 35PDMPA that contains rings and heteroatoms obtained from:

$$\sigma^2 = \langle R_0^2 \rangle \langle R_{of}^2 \rangle^{-1} \quad (8)$$

The mean square unperturbed end-to-end distance, $\langle R_0^2 \rangle$ obtained experimentally from the value of K_0 , which is related to the rigidity factor, σ , or to the Flory's characteristic ratio, C_∞ , by the expressions:

$$\sigma = \left(\frac{\langle R_0^2 \rangle}{\langle R_{of}^2 \rangle} \right)^{1/2} = \left(\frac{K_\theta}{\Phi_0} \right)^{1/3} \left(\frac{M_0}{4l^2} \right)^{1/2} \quad (9)$$

$$C_\infty = \frac{\langle R_0^2 \rangle}{\langle R_{00}^2 \rangle} = \left(\frac{K_\theta}{\Phi_0} \right)^{2/3} \frac{M_0}{2l^2} = 2\sigma^2 \quad (10)$$

where M_0 is the molecular mass of the monomer and the number of C-C bonds in the chain: $n = 2M/M_0$. The values of σ and C_∞ based on Eqs (9) and (10) are also tabulated in the Table 2.

Comparison with 35PDMPMA and PMA helps to understand the Stockmayer-Fixman plot. The $\sigma = 3.15$ in toluene obtained from extrapolation of higher molar mass data; it is lower than $\sigma = 3.82$ of 35PDMPMA in toluene and higher than $\sigma = 2.17$ of PMA in toluene at 40°C as expected. Therefore, this must be the best σ describing the nature of 35PDMPA. However, the value of $\sigma = 2.50$ obtained from the intercept of plot of extrapolation of data at lower molar mass region similar to the σ obtained from intercept of second order polynomial as well as the one considering all points are underestimated values. These values are in the range of σ of a very flexible polymer chain such as PMA not a hindered one such as 35PDMPA. Structurally, 35PDMPA is more rigid than PMA these low values of σ must be the result of underestimation of K_θ by extrapolation at lower molar mass regions.

Two different factors may contribute in determining a high value of σ for a polymeric chain: the nature of the main chain and the effects of side chains. In case of 35PDMPA, the nature of the main chain, which is composed of a simple hydrocarbon chain, may not contribute to the σ as the hindered voluminous side di-metha-phenyl ester groups. The 3,5-dimethylphenyl lateral chains occupy a large volume and hinder the backbone internal rotations by establishing orientational correlations between themselves.

The stiffening of the polymer chain due to the presence of large aromatic groups and long n-alkyl pendant groups has already been reported for some other polymers by several researchers.⁴⁻⁶ Also, it is known that the interaction of elements of polymer chains with solvent molecules could affect the probability distribution of the angles of internal rotation in the chain.²⁶ This observation was confirmed both theoretically²⁷⁻²⁸ and experimentally.³

The value of C_∞ of 35PDMPA (19.85) obtained from the plateau of the points at higher molar mass is much within expectation. The C_∞ values observed for many atactic vinyl polymers are in the range of $5 < C_\infty < 10$ usually found in the literature.⁴ The C_∞ values observed for PMA in toluene is 9.43; and the one of polyphenylmethacrylate, PPMA, both theta solvents and good solvents ranges 12.2 and 13.3. The PPMA's C_∞ is found to be ~50% larger than that of atactic PMA. Therefore, a C_∞ value smaller than that of 35PDMPMA (29) is expected for 35PDMPA.

It should also be remarked that the value of C_∞ in good solvents probably has been underestimated as they were obtained by extrapolating to $M=0$ the molecular weight region of Stockmayer-Fixman plot in which the effect of stiffness is coupled with excluded volume. However, chain rigidity may be contributing to the slope so that the results obtained for K_θ and C_∞ could be inaccurate. An indication that the positive slope in this plot may include the effect of chain stiffness comes from the convergent trend observed in the curves at high molecular weights.

4. Conclusion

It is common to consider the equilibrium flexibility of macromolecules in a solution based on the value of the conformational parameter $\sigma = (\langle R_0^2 \rangle / \langle R_{0f}^2 \rangle)^{1/2}$. The σ for 35PDMPA yields 3.15 (see Table 2); such a high value of σ does not necessarily imply that the state of internal rotation of units in 35PDMA chains is truly hindered in view of the fact that the 35PDMPA chain backbone look like a polyethylene chain but contains 3,5-dimethylphenyl-esters groups as side chains. But this means that the parameter σ has meaning only for chain molecules with flexibility imparted by rotation around valence bonds without distortion of valence angles by side chain groups, therefore, σ is unsuitable for use with many polymers, especially those containing a hindered side chains such as 35PDMPA, those whose angle of rotation may be hindered by polymer-solvent interactions and those that have cyclic structures in the chain backbone.

Notes

1. Terao, Ken, Mays, Jimmy W. *European Polymer Journal* 40 (2004) 1623–1627
2. Ikeda, Hiroaki and Shima, Hiroyuki *Eur Polym J* 40 (2004) 1565-1574
3. Stockmayer WH, Fixman M. *J Polym Sci* 1961;C1:137; Stockmayer WH, Fixman M. *J Polym Sci* 1976:1125; Yamakawa H. *Modern theory of polymer solutions*. New York: Harper & Row, Publishers; 1971.
4. Cowie, J.M.G. *Polymers: Chemistry & Physics of Modern Materials*, Chapman & Hall, London, 2nd edn. (1991). (1a) pp. 165, 191-192 and 219; (1b) p 217, (1c) P 218
5. Flory, P. J. *Principles of Polymer Chemistry*, Cornell University Press, Ithaca, NY (1953) 2a p 27, 2b p 310, (3c) P. 617.
6. Yamakawa, H. *Modern Theory of Polymer Solution*, Harper and Row Publishers, New York, (1971).
7. Chi, Wu and Gong Xiangjun *Encyclopedia of Polymer Science and Technology, Laser Light Scattering: Some Recent Developments 2010* by John Wiley & Sons
8. Flory, P. J. *Statistical Mechanics of Chain Molecules*, Interscience, New York (1969)
9. Zhongde x, Hadjichristidis N, Fetters L.J. *Macromolecules* 1984, 14, 2303-2306
10. Gargallo, L.; Hamidi, N.; Radic, D., *Polymer*, **31**, 924 (1990)
11. Flory PJ, Abe Y. *Macromolecules* 1971, 4, 219-230
12. Yamakawa, H. and Fuji, M., *Macromolecules* **7**(1), 128-135(1974).
13. Bohdanecký, M., *Macromolecules* 16, 1483 (1983).
14. Fritz, G.; Scherf, G.; Glatter, O. 2000 (104)
15. Hong, Fei, Yijie Lu, Junfang Li, Wenjing Shi, Guangzhao Zhang, and Chi Wu *Polymer* 51 (2010) 1413–1417
16. Le Guillou, J. C. and Zinn-Justin, J.J. *Phys. Rev. Lett.* 1977, 39, 95
17. Davidson, N. S., Fetters, L. J., Funk, W. G., Hadjichristidis, N and Graessley, W. W. *Macromolecules* 1987, 20, 2614-2619
18. Adam, M.; Delsantim M. *Macromolecules* 1977. 10, 1229
19. Matsuoka, S; M.K. Cowman *Polymer* 43 (2002) 3447-3453
20. Liu, Guojun, Xiaohu Yan, Scott Duncan *Macromolecules* **2003**, 36, 2049-2054
21. Barrales-Rienda, J. M.; Romero Galicia, C.; Horta, A. *Macromolecules*, **16**, 1707 (1983).
22. Tonelli, A. E. *NMR Spectroscopy and Polymer Microstructure, The Conformational Connection*, VHC publishers, New York, NY 10010 (1989) P. 56
23. Yamakawa, H. and Fuji, M., *Macromolecules* **7**(1), 128-135(1974).
24. Miyaki, Y.; Einaga, Y.; Fujita, H.; Fukuda, M., *Macromolecules* **13**, 588-592 (1980)
25. D. Radic, F. Martinez, L. Gargallo, and N. Hamidi, "Synthesis and Characterization of Bulky Side Chain Methacrylate Polymers," *Polym. Eng. Sci.*, **36**(2), 188-193 (1996).
26. Lifson, S. and Oppenheim, I., *J. Chem. Phys.* **33**, 109 (1960)
27. Joon, D. J. ; Sundarajan, P. R. and Flory, P. J. *Macromolecules* **8**, 776 (1975)
28. Beha, T. and Valko, L., *Polymer* **17**, 298 (1976)